Parametric study of thorium fuel cycles in a 100MW$_{th}$ pebble bed high temperature reactor

F Panday

Mini-dissertation submitted in partial fulfilment of the requirements for the degree Master of Science in Nuclear Engineering at the Potchefstroom Campus of the North-West University

Supervisor: Prof. E. Mulder
Co-supervisor: Mr. D. Serfontein

May 2011

ABSTRACT

The current project was conducted in order to select an optimized open Thorium/Uranium fuel cycle for the Pebble Bed Modular Reactor (PBMR) concept in motivation for the 100MW_{th} PBMR Power Plant. A sensitivity study on the heavy metal loading of the fuel sphere was performed to accomplish this task. The effect on various parameters was evaluated to determine the influence of varying the Heavy Metal (HM) from 6 gHM/sphere to 20 gHM/sphere and at different feed fuel enrichments from 6 to 18 wt%.

The findings also gave insight into the fuel cycle performance and the Uranium ore savings that is envisaged. The 20 gHM/sphere HM loading performed the best amongst the other HM fuel loadings. It also showed the least Uranium ore requirement namely; 15 % less than that required by the Uranium cycle. Recommendations for further research based on the results obtained in the study, are made in the closing chapters.

I, the undersigned, hereby declare that the work contained in this project is my own original work.

_____
F Panday

May 2011
Centurion

Dedication

In memory of my loving sister

Nivisha Panday

06/06/1979 – 06/07/1998

Acknowledgments

The All Mighty that gave me the strength to accomplish my task.

The staff at North-West University.

My family and colleagues at PBMR Ltd, for their moral support.

Table of Contents

1.INTRODUCTION 1
- **1.1 Background 1**
- **1.2 Literature Review 3**
- **1.3 Main Objectives 9**
- **1.4 Structure of Mini-Dissertation 10**
- **1.5 Notation 11**

2.THEORY 12
- **2.1 The General Form of the Boltzmann Equation [12] 12**
- **2.2 Aspects of Diffusion Theory of Neutron Transport [11] 13**
  - 2.2.1 The Diffusion Equation 13
  - 2.2.2 Finite Difference Solution of the Diffusion Equation 15
  - 2.2.3 Boundary Conditions 15
- **2.3 Physics, Limitations in Fuel Element, Reactor and Fuel Cycle 18**

3.CALCULATION METHODOLOGY 20
- **3.1 Introduction 20**
- **3.2 V.S.O.P.-A Computer Code System 20**
- **3.3 Geometry 24**
  - 3.3.1 Geometrical Layout in V.S.O.P.-A 24
- **3.4 Calculation Methodology 25**
- **3.5 Model Adjustments and Execution of Code 26**
  - 3.5.1 Calculation of Resonance Integrals 26
  - 3.5.2 Execution of Resonance Integral 27
  - 3.5.3 Preparation of Volume Matrix 27
  - 3.5.4 Execution of Volume Matrix 27
  - 3.5.5 Calculation of V.S.O.P.-A 28
  - 3.5.6 Execution of V.S.O.P.-A 28
  - 3.5.7 Calculation of THERMIX 28
  - 3.5.8 Execution of THERMIX 29

4.EVALUATION OF CALCULATIONS, RESULTS AND DISCUSSION 30
- **4.1 Extraction of Data from V.S.O.P.-A Output Files 30**
- **4.2 Evaluation of the Calculations 30**
- **4.3 Results and Discussion 31**
- **4.4 Discussion Summary 44**

5.CONCLUSIONS AND RECOMMENDATIONS 45

6.BIBLIOGRAPHY 46

7.APPENDICES 48
- **7.1 Appendix A: Data for Fuel Supply and Discharge 48**
- **7.2 Appendix B: Data for ISU and Fraction of Fissions in Bred Fissile Nuclides 50**

Abbreviations

Abbreviation or Acronym	Definition
AVR	Arbeitsgemeinschaft Versuchs-Reaktor
Bi	Bismuth
BWR	Boiling Water Reactor
eV	Voltage (electric)
FA	Fractional Absorption
FIFA	Fissions per Initial Fissile Atoms
HEU	High Enriched Uranium
HM	Heavy Metal
HTRs	High Temperature Reactors
ISU	In-Situ Utilization
k_{eff}	Effective multiplication factor (criticality)
k_{∞}	Infinity multiplication factor (criticality)
LEU	Low Enriched Uranium
MW_{th}	Megawatt (thermal)
MW_e	Megawatt (electric)
OTTO	Once Through Then Out
PBMR (Pty) Ltd	Pebble Bed Modular Reactor (Propriety) Limited
Pu	Plutonium
PHWRs	Pressurised Heavy Water Reactors
PWRs	Pressurized Water Reactors
RUDI-1	Reactor name
SiC	Silicone Carbide
Th	Thorium
ThO_2	Thorium Dioxide
Tl	Thallium
THTR	Thorium High Temperature Reactor
U	Uranium
UO_2	Uranium Dioxide
UK	United Kingdom
USA	United State of America
V.S.O.P.-A	Very Superior Old Programs (Advanced)
wt %	Weight Percentage (enrichment)
ZUT-DGL	Computer Program to calculate the unresolved resonance integrals
℃	Degree Celsius

List of Figures

Figure 1: The Thorium Decay Chain [7] 7
Figure 2: The Uranium Decay Chain [8] 8
Figure 3: Representation of Flux at Problem Boundary 16
Figure 4: V.S.O.P. Physics Simulation [21] 21
Figure 5: V.S.O.P. - The Basic Programs [21] 23
Figure 6: V.S.O.P.-A Calculation Model 25
Figure 7: U_3O_8 Requirement as a function of Heavy Metal Loading 32
Figure 8: Conversion Ratio as a function of Heavy Metal Loading 33
Figure 9: Average Burn up as a function of Heavy Metal Loading 34
Figure 10: In-Situ Utilization of Bred Fissile Nuclides as a function of Heavy Metal Loading 35
Figure 11: Fraction of Fissions in the Bred Fissile Nuclides as a function of Heavy Metal Loading 36
Figure 12: Fuel Residence Time as a function of Heavy Metal Loading 37
Figure 13: Separative Work as a function of Heavy Metal Loading 42
Figure 14: Core Leakage as a function of Heavy Metal Loading 43

List of Tables

Table 1: Approximate Nuclear Properties in a HTR – Neutron Spectrum 3
Table 2: Notation Used 11
Table 3: Geometrical Specifications of Pebble Bed Reactor 'RUDI-1' 24
Table 4: Performance of U/Th Fuel Cycle at 6 wt % Feed Fuel Enrichment 38
Table 5: Performance of U/Th Fuel Cycle at 9 wt % Feed Fuel Enrichment 39
Table 6: Performance of U/Th Fuel Cycle at 13 wt % Feed Fuel Enrichment 40
Table 7: Performance of U/Th Fuel Cycle at 18 wt % Feed Fuel Enrichment 41

1. INTRODUCTION

1.1 Background

In order to ensure future nuclear sustainability, the world's finite Uranium (U) resources need to be preserved [1]. The Thorium (Th) fuel cycle has been playing a dominant role in High Temperature Reactors (HTRs) due to the favourable nuclear properties of the bred U-233 [2]. A parametric study of Th fuel cycles is proposed by varying the heavy metal loadings per fuel sphere in order to provide an overview of the various characteristics observed in comparison to the Uranium reference cycle.

A 100 MW_{th} Pebble Bed Modular Reactor (PBMR) has been proposed by Mulder *et al* at the Post Graduate School for Nuclear Science and Engineering, North-West University [3]. This reactor has been conceptualized for the Low Enriched Uranium (LEU) fuel cycle of 9.6 wt% enrichment in U-235. In the reference cycle the bred fissile Plutonium (Pu) isotopes are predominantly burnt in-situ in the reactor, and only 16 % have been estimated to appear in the spent fuel spheres [3].

This concept features the fuel elements circulating only once through the core in a so-called, Once Through Then Out (OTTO) cycle. The loading of about 260 spheres per day can be inserted into the top of the core in regular intervals of one or more days. This leads to considerable simplification of the fuelling and fuel handling features of this type of reactor. Also OTTO cycle aims to achieve maximum power as possible from the feed fuel. The fuel sphere is moved only once at a slow rate from the top to bottom through of the reactor. There is a depletion of fuel towards the lower section of the core, resulting in an axial tilt of the power density. Also the downward movement of the cooling gas enables optimal removal of heat from the reactor. The coolant experiences pressure drop, Δp, as it flows through the fuel channels in a reactor.

The pressure drop in a pebble bed reactor is given as [4]:

$$\Delta p = \Psi \cdot \frac{1-\varepsilon}{\varepsilon^3} \cdot \frac{H}{d_{ball}} \cdot \frac{1}{2\rho} \cdot \left(\frac{\dot{m}}{A}\right)^2$$

Where A = cross-section of the core

d_{ball} = pebble diameter

H = height of the pebble bed

$\dot{m}$ = mass fow of the helium

Δp = pressure drop

ε = void fraction

ρ = helium density

Ψ = frictional loss parameter

$$\psi = \frac{320}{\frac{Re}{(1-\varepsilon)}} + \frac{6}{\left(\frac{Re}{(1-\varepsilon)}\right)^{0.1}}$$

$$Re = \frac{\dot{m} \cdot d_{hall}}{A \cdot \eta}$$

and

$$1 \leq \frac{Re}{1-\varepsilon} \leq 10^5$$

$$0.36 \leq \varepsilon \leq 0.42$$

The coolant flows from a higher pressure and power density to a lower pressure and power density in the reactor core. The coolant temperature in the bottom of the reactor is at a higher temperature due to the heat-up over the height of the pebble bed core. The coolant flows from a lower temperature to a higher temperature resulting in the overall heat transfer flow in the reactor. Heat removal in normal operation is exclusively due to heat transfer to the coolant. Power level and heat removal in the reactor can be controlled by changing the coolant flow rate through the reactor. There exists an area of high power density in the upper section of the core.

1.2 Literature Review

Over the last 50 years there has been keen interest in Thorium research, especially because it can be utilized as nuclear fuel in a similar manner that Uranium has been used to fuel nuclear reactors [5]. Thorium is found in small amounts in the earth's crust. It is almost three times more abundant in nature than Uranium [2]. It was discovered in 1828 by the Swedish chemist Jons Jakob Berzelius [2]. Thorium is not fissile but the Th-232 will absorb thermal and epithermal neutrons to produce U-233 which is a fissile and long lived material. In one significant respect U-233 is better than U-235 and Pu-239, i.e. because of a higher probability of fission and a higher neutron yield per neutron absorbed (η). Performance of the different fuel cycles is determined by the nuclear properties of the involved nuclides Table 1.

Table 1: Approximate Nuclear Properties in a HTR – Neutron Spectrum

		^{232}Th	^{238}U		
Resonance integral	barn	50	89		
Thermal absorption cross section	barn	2.7	1.1		
		^{233}U	^{235}U	^{239}Pu	^{241}Pu
Neutron absorption per fission	1+α	1.12	1.24	1.59	1.41
Neutron production per absorption	η	2.24	1.98	1.81	2.10
Thermal absorption cross section	barn	250	230	1100	900

Th-232 decays very slowly (its half-life is about three times the age of the Earth) but other Thorium isotopes occur in its' and in Uranium's decay chains [2]. Most of these are short-lived and hence much more radioactive than Th-232, though on a mass basis they are negligible [2].

Thorium Dioxide (ThO_2), also called Thoria, has one of the highest melting points of all oxides, approximately 3300℃. Because of these properties, Thorium has found applications in light bulb elements, lantern mantles, arc-light lamps, welding electrodes and heat-resistant ceramics [2].

The most common source of thorium is the rare earth phosphate mineral, Monazite, which contains up to about 12% Thorium Phosphate, but 6-7% on average [2]. Monazite is found in igneous and other rocks. World Monazite resources are estimated to be about 12 million tonnes, two thirds of which are in heavy mineral sands deposits on the South and East coasts of India. Thorite ($ThSiO_4$) is another common mineral. A large vein deposit of Thorium and rare earth metals is in Idaho [2].

As alluded to above the use of Thorium based fuel cycles has been studied for more than 50 years, but on a much smaller scale than Uranium or Uranium/Plutonium cycles. Basic research and development has been conducted in Germany, India, Japan, Russia, the United Kingdom (UK) and the United States of America (USA). Test reactor irradiation of Thorium fuel to high burn-ups has also been conducted and several test reactors have either been partially or completely loaded with Thorium based fuel [2].

Some of the main benefits of Thorium are as follows:

- Thorium is 3 to 4 times more abundant in the world than Uranium [6].
- Thorium fuel cycle is an attractive way to produce long term nuclear energy with low radiotoxicity waste [6].
- Thorium Dioxide (ThO_2) is chemically more stable and has higher radiation resistance than Uranium Dioxide (UO_2) [6]. The fission product release rate for ThO_2 based fuels are one order of magnitude lower than that of UO_2. ThO_2 has favourable thermo-physical properties because of the higher thermal conductivity and lower coefficient of thermal expansion compared to UO_2. Thus, ThO_2 based fuels are expected to have better in-pile performance than that of UO_2 and UO_2 based mixed oxide.
- Excellent past performance of ThO_2, $(Th,U)O_2$, ThC and (Th,U)C fuels in HTRs in Germany, USA and UK [6].
- Intrinsic proliferation resistance of Th-232 and bred U-233 fuel cycle.
- In-situ burning of Plutonium of thermal neutron reactors in an “OTTO” cycle.
- Highly enriched Uranium allowed more compact cores, with high neutron fluxes and also longer times between refuelling.

However Thorium also has a few challenges that need to be overcome, these are namely [2]:

- The irradiated Th or Th-based fuels contain significant amount of U-232 with a half-life of only 73.6 years. The U-233 is associated with strong gamma emitting daughter products, Bismuth (Bi-212) and Thallium (Tl-208) with very short half-lives. There is significant buildup of radiation dose with storage of spent Th based fuel or separated U-233, which requires remote and automated reprocessing and re-fabrication in heavily shielded hot cells and results in an increase in the cost of fuel cycle activities. This is, however, viewed to provide the intrinsic proliferation properties to this fuel cycle.
- The use of HEU may also pose as a proliferation risk. Appropriate safety and security precautions must be in place to mitigate the risk. However it still remains questionable whether nuclear regulators will allow the use of HEU, especially outside the Nuclear Weapons States.

Research and development experiments involving Thorium, either as block or as pebble fuel, include the following [2]:

- Thorium fuel elements with a 10:1 Th/U(HEU) ratio were irradiated in the 20 MW_{th} Dragon reactor at Winfrith, UK, for 741 full power days [2]. Dragon was run as an OECD/Euratom cooperation project, involving Austria, Denmark, Sweden, Norway and Switzerland in addition to the UK, from 1964 to 1973. The Th/U fuel was used to 'breed and feed', so that the U-233 formed replaced the U-235 at about the same rate, and fuel could be left in the reactor for about six years.
- Between 1967 and 1988, the AVR (Arbeitsgemeinschaft Versuchs-Reaktor) experimental pebble bed reactor at Jülich, Germany, operated for over 750 weeks at 15 MW_e, about 95% of the time with Thorium based fuel [2]. The fuel used consisted of about 100,000 billiard ball-sized fuel elements. Overall a total of 1360 kg of Thorium was used, mixed with High Enriched Uranium (HEU). Burn-ups of 150,000 MWd/t were achieved [2].
- General Atomics' Peach Bottom high-temperature, graphite-moderated, helium-cooled reactor in the USA operated between 1967 and 1974 at 110 MW_{th}, using HEU with Thorium [2].

• In India, the Kamini 30 kW_{th} experimental neutron-source research reactor using U-233, recovered from ThO_2 fuel irradiated in another reactor, started up in 1996 near Kalpakkam [2]. The reactor was built adjacent to the 40 MW_{th} Fast Breeder Test Reactor, in which the ThO_2 is irradiated.

• In the Netherlands, an aqueous homogenous suspension reactor has operated at 1 MW_{th} for three years [2]. The HEU/Th fuel is circulated in solution and reprocessing occurs continuously to remove fission products, resulting in a high conversion rate to U-233. The proliferation risk of such a configuration is very high. This is because pure U-233 can be removed from the reactor continuously before the actual formation of the highly radioactive U-232 can take place.

Much experience has been gained in Thorium based fuel in power reactors around the world, some using HEU as the main fuel [2]:

• The 300 MW_e Thorium High Temperature Reactor (THTR) in Germany was developed from the AVR and operated between 1983 and 1989 with 674,000 pebbles, over half containing Th/HEU fuel (the rest graphite moderators and some neutron absorbers) [2]. These were continuously recycled on load and on average the fuel passed six times through the core.

• The Fort St Vrain prismatic block fuel reactor was the only commercial Thorium fuelled nuclear plant in the USA, also developed from the AVR in Germany, and operated 1976-1989 [2]. It was a high temperature (700℃), graphite-moderated, helium-cooled reactor with a Th/HEU fuel designed to operate at 842 MW_{th} (330 MW_e). The fuel was in microspheres of Thorium Carbide and Th/U-235 carbide coated with Silicon Oxide and Pyrolytic Carbon to retain fission products. It was arranged in hexagonal columns (prismatic blocks) rather than as pebbles. Almost 25 tonnes of Thorium was used in fuel for the reactor, and this achieved 170,000 MWd/t burn-up [2][9].

• Thorium based fuel for Pressurized Water Reactors (PWRs) was investigated at the Shippingport reactor in the USA [2].

• In India, thorium has been used for power flattening in the initial cores of the two Kakrapar Pressurised Heavy Water Reactors (PHWRs) [2].

• The 60 MWe Lingen Boiling Water Reactor (BWR) in Germany utilized Th/Pu based fuel test elements [2].

Figure 1 depicts the Thorium decay chain and Figure 2 the Uranium decay chain

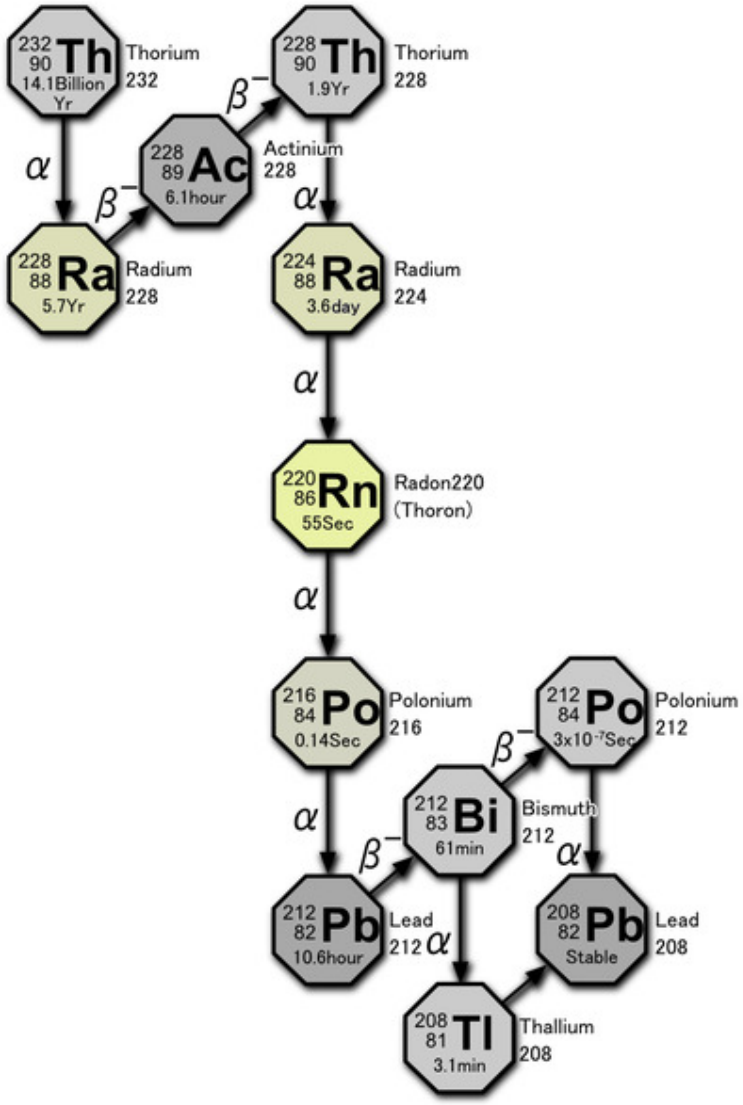


Figure 1: The Thorium Decay Chain [7]

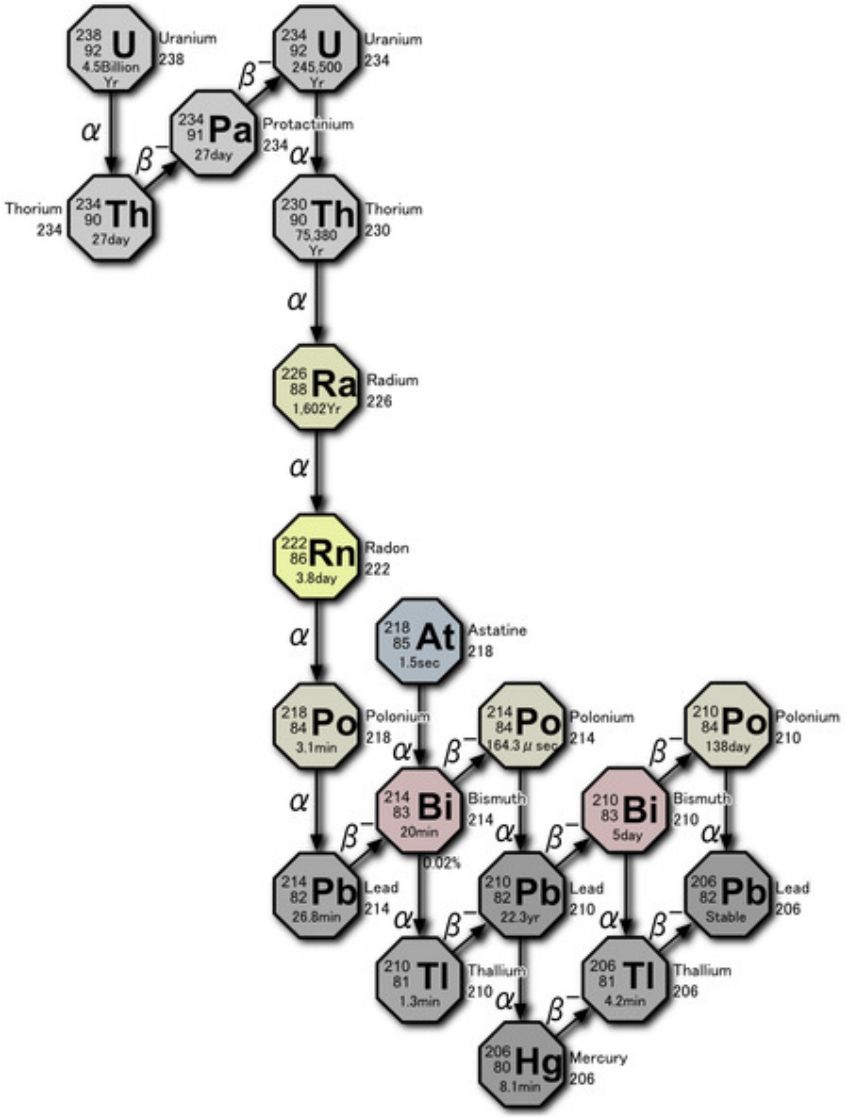


Figure 2: The Uranium Decay Chain [8]

A total fuel cycle model must be developed in order to determine the economic viability of the cycle. These costs include, but are not limited to, the following:

- the cost of fabrication,
- waste disposal cost, chemical reprocessing, etc.

The key to achieving good fuel performance lies in the correct choice of materials [10], namely:

- high density Oxidic kernel,
- low density buffer layer derived from Ethyne,

- TRISO coating, i.e., the sequence Pyrocarbon, Silicon Carbide (SiC), Pyrocarbon,
- Low temperature Isotropic Pyrocarbons derived from Propene,
- high quality SiC of near theoretical density derived from Methyltrichlorosilane.

The high degree of safety of HTRs results from the ability of the TRISO coated fuel particles to retain fission products even at high temperatures. Small modular HTRs are designed in such a way that maximum fuel temperatures during severe accidents remain below about 1600℃ without the need for active control mechanisms [10]. In simulations of normal and transient operation, and in accidents not exceeding 1600-1700℃, it was demonstrated that all radiologically relevant fission products namely; Iodine, Caesium, and Strontium, are almost completely retained inside the SiC layer of intact fuel particles [10].

1.3 Main Objectives

The main objective of this project is to determine the optimal HM loading per fuel sphere for the Thorium fuel cycles in a 100 MW_{th} pebble bed configuration by comparing them to the Uranium reference fuel cycle. The criteria used to achieve the main objective are:

I. Determination of the Uranium ore consumption per fuel cycle for the different HM loadings,
II. Determination of the effect of varying the feed fuel enrichment on the Uranium ore consumption per fuel cycle,
III. Determination of the conversion ratio (average number of fissile atoms produced in a reactor per fissile fuel atom consumed) for each fuel cycle,
IV. And determination of the in-situ utilization of bred fissile nuclides in the fuel cycle.

The conclusions derived by investigating the criteria namely; Uranium ore savings, burn-up, overall fuel cycle performance etc, would then lead to determining the optimal Thorium fuel cycle.

The enrichment in Uranium (U-235/(U-235 + U-238)) is 93%. The enrichment in feed fuel is varied from 6 wt % to 18 wt %. The wt% is U-235 versus heavy metal including the Thorium. The fuel is loaded in $(Th+U)O_2$ mixed oxide coated particles.
The investigation assumes no reprocessing facilities are available so no credit is given for spent fuel.

1.4 Structure of Mini-Dissertation

The dissertation is presented in seven chapters, including this introduction chapter and the last chapter, which contains the appendices.

Chapter 2 describes the theory of Very Superior Old Programs (Advanced version) (V.S.O.P.-A) that was used to model the different cases for the sensitivity study. There is an emphasis on diffusion theory, which is applicable in the V.S.O.P.-A code. Other relevant theory is also given.

Chapter 3 focuses on the calculation methodology used to arrive at the results and output files. A short description of the input files to V.S.O.P.-A and the input cards that were changed for the different models are given. The method of running V.S.O.P.-A codes is also discussed.

Chapter 4 details the evaluation of the calculations, the results of the sensitivity study, and also provides a discussion of the results obtained from the analysis of the output files.

The conclusion of this project is presented in Chapter 5. It includes recommendations on the current study and possible further work that may provide more useful insight into the Thorium fuel cycle.

Chapter 6 is the Bibliography of references used in this project.

The appendices are given in Chapter 7, with some of the raw data used in the project.

1.5 Notation

The notations used are given in Table 2.

Table 2: Notation Used

D	Diffusion constant
k_{eff}	Effective multiplication factor
α	External extrapolated boundary constant
$\tilde{a}$	Extrapolation length
$J_-\ J_+$	Inward and outward partial currents, respectively
$\Sigma_t(\vec{r},E)$	Macroscopic transfer cross section, in this instance it is the total macroscopic cross section for energy E
Δ	Mesh spacing
$\psi(\vec{r},E,\vec{\Omega})$	Angular Neutron Flux at position $\vec{r}$, with energy E and in direction $\vec{\Omega}$
ρ	Reactivity
λ_{tr}	Transport length

2. THEORY

In depth theory on nuclear reactor physics, fuel cycles and other related topics can be found in references [11], [12] and [13].

2.1 The General Form of the Boltzmann Equation [12]

The time-independent Boltzmann transport equation that describes the neutron balance in a reactor can be written as

$$\vec{\Omega} \cdot \nabla \psi(\vec{r}, E, \vec{\Omega}) + \Sigma_t(\vec{r}, E)\psi(\vec{r}, E, \vec{\Omega}) = S(\vec{r}, E, \vec{\Omega}) \quad (1)$$

This expression states that the losses due to leakage and collisions must be equal to the source of neutrons, at some point in space $\vec{r}$ with energy E and direction $\vec{\Omega}$. In this expression, $\Sigma_t(\vec{r}, E)$ is the total macroscopic cross section at energy E of the medium, which is typically assumed isotropic, and $\psi(\vec{r}, E, \vec{\Omega})$ is the angular flux.

The source term, $S(\vec{r}, E, \vec{\Omega})$ has three components:

a scattering source term $S'(\vec{r}, E, \vec{\Omega})$

a fission source term $F(\vec{r}, E, \vec{\Omega})$ and

a fixed source term, $Q(\vec{r}, E, \vec{\Omega})$.

The scattering source term is given by

$$S'(\vec{r}, E, \vec{\Omega}) = \int_0^{4\pi} d\vec{\Omega}' \int_0^{\infty} dE' \Sigma_s(\vec{r}, E' \to E, \vec{\Omega}' \to \vec{\Omega})\psi(\vec{r}, E', \vec{\Omega}'). \quad (2)$$

The fission source term can be written as

$$F(\vec{r}, E, \vec{\Omega}) = \frac{1}{4\pi k} \chi(\vec{r}, E) \int_0^{4\pi} d\vec{\Omega}' \int_0^{\infty} dE' \nu(\vec{r}, E') \Sigma_f(\vec{r}, E')\psi(\vec{r}, E', \vec{\Omega}'). \quad (3)$$

where

$\Sigma_s(\vec{r}, E' \to E, \vec{\Omega}' \to \vec{\Omega})$ is the macroscopic double differential scattering cross section per unit energy for scattering from energy E' to E and direction $\vec{\Omega}'$ to $\vec{\Omega}$,

$\chi(\vec{r},E)$ is the fraction of the fission neutrons per unit energy produced at $\vec{r}$ and E,

$\nu(\vec{r},E)$ is the average number of neutrons produced per fission,

$\Sigma_f(r,E)$ is the macroscopic fission cross section and

k is the "effective multiplication factor."

2.2 Aspects of Diffusion Theory of Neutron Transport [11]

2.2.1 The Diffusion Equation

The transport equation, eq 1, can be written in the diffusion theory formalism if the following assumptions can be made about the system under consideration [13].

- The flux is assumed to be sufficiently slowly varying in space,

- absorption is small relative to scattering, and

- Fick's law holds in the following form:

$$\vec{J} = -D\nabla\phi \tag{4}$$

where D is the diffusion constant.

Then a basic equation expressing the diffusion approximation to neutron transport at some location $\vec{r}$ and energy E can be written as [14]

$$\begin{aligned} &-\nabla D(r,E)\nabla\phi(r,E) + (\Sigma_a(r,E) + \Sigma_s(r,E))\phi(r,E) \\ &= \int_{E'} dE' \left(\Sigma_r^{E'\to E} + \frac{\chi(E)\nu\Sigma_f(r,E')}{k} \right) \phi(r,E') \end{aligned} \tag{5}$$

Eq 5 can be simplified to eq 6 when the following is done:

- the continuous energy spectrum is divided into discrete energy groups

- a buckling term is allowed when appropriate

- the source distribution function $\chi(E)$ is assumed to have no spatial dependence

- a simplification is made in the transport term

$$
\begin{aligned}
&-D_g(r)\nabla^2\phi_g(r)+\left(\Sigma_a^g(r)+\sum_n\Sigma_s^{g\to n}(r)+D_g(r)B_g^2\right)\phi_g(r)\\
&=\sum_n\left(\Sigma_s^{n\to g}(r)+\frac{\chi_g\nu\Sigma_f^n(r)}{k}\right)\phi_n(r)
\end{aligned}
\qquad (6)
$$

In this equation, ∇^2 is the Laplacian geometric operator,

$\phi_g(r)$ is the scalar neutron flux at location $\vec{r}$ and in energy group g,

$\Sigma_a^g(r)$ is the macroscopic cross section for absorption, normally weighted over a representative flux energy spectrum,

$\Sigma_s^{g\to n}(r)$ is the macroscopic cross section for scattering of neutrons from energy group g to energy group n,

$D_g(r)$ is the diffusion coefficient, normally one-third of the reciprocal of the transport cross section,

B_g^2 is the buckling term to account for the effect of the Laplacian operator (leakage) in a dimension not treated explicitly,

$\nu\Sigma_f^g(r)$ is the macroscopic production cross section, (ν) is the number of neutrons produced by a fission and Σ_f is the cross section for fission,

χ_g is the distribution function for source neutrons, and

k is the effective multiplication factor, ratio of rate of production of neutrons to rate of loss of neutrons from all causes, an unknown to be determined.

2.2.2 Finite Difference Solution of the Diffusion Equation

In order to solve eq 6, one approach is to solve the equation numerically using a standard finite difference formulation. Here, a mesh is established in the spatial geometry, where each point of the mesh is a point for the numerical analogue of eq 6. The Laplacian operator ∇^2 with respect to a given point is written in the usual manner in terms of the neighbours of the point. An iterative procedure incorporating energy group–to-group coupling is then carried out to determine the fluxes at the spatial mesh points for all the energy groups.

2.2.3 Boundary Conditions

To obtain a solution using the finite difference method, boundary conditions must be established at the boundaries of the system. Mathematically, this amounts to setting the number of equations available to be equal to the numbers of unknowns that must be solved. The boundary equations in this case are specified by the external extrapolated boundary constant, α .

To establish the origin of α , consider a mesh that lies on a given boundary, and for brevity, assume that this is an external boundary. Let ϕ_c be the internal flux in this mesh at some internal point, typically chosen to be the centre, ϕ_a to be the flux on the boundary, and Δ to be the distance from the internal point to the boundary.

Given the slope of the flux at the boundary, a point will exist at a distance $\tilde{a}$ from the boundary at which the flux can be extrapolated to zero, irrespective of whether void or material exists beyond the boundary.

From Figure 3 the slope m at the boundary can be written as

$$m = \frac{\phi(a+\tilde{a})-\phi(a)}{(a+\tilde{a})-a} = \frac{0-\phi(a)}{a+\tilde{a}-a} = -\frac{\phi(a)}{\tilde{a}} = -\frac{\phi_a}{\tilde{a}}$$

i.e.,

$$m = -\frac{\phi_a}{\tilde{a}} \tag{7}$$

Also, by definition of the gradient,

$$m = \left.\frac{d\phi}{dx}\right|_{x=a} \tag{8}$$

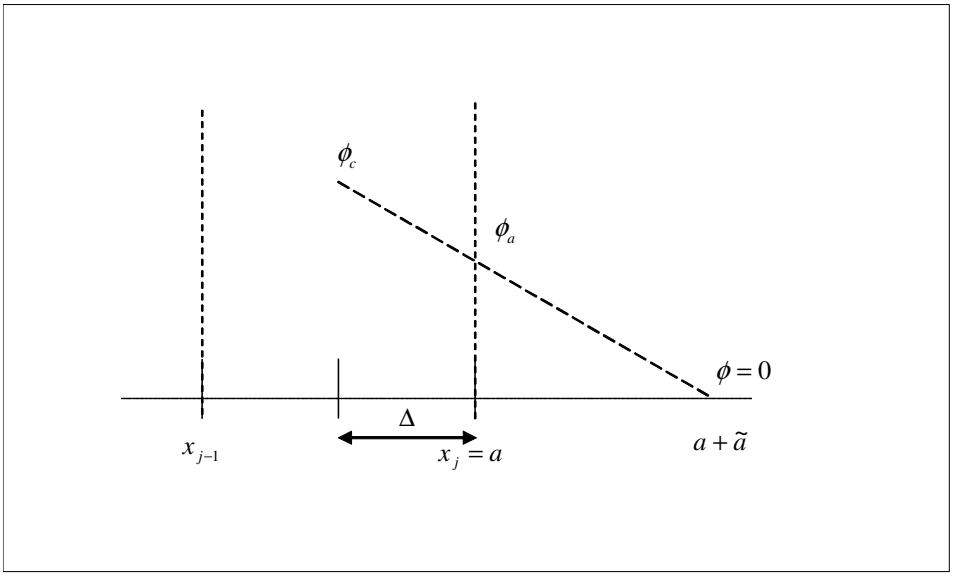


Figure 3: Representation of Flux at Problem Boundary in Finite Difference Approach

Equating 7 and 8 we get

$$-\frac{\phi_a}{\tilde{a}} = \left.\frac{d\phi}{dx}\right|_{x=a}$$

Rearranging this becomes

$$-\frac{d\phi/dx\big|_{x=a}}{\phi_a} = \frac{1}{\tilde{a}} \tag{9}$$

However, we can also write the gradient at boundary as

$$-\frac{\partial\phi}{\partial x} = \frac{\phi_c - \phi_a}{\Delta} \tag{10}$$

Thus, from eq 10 and 9 we get the boundary condition

$$\frac{\phi_c - \phi_a}{\Delta} = -\frac{\phi_a}{\tilde{a}} \tag{11}$$

which, when used in the finite difference formulation, is the equation needed to complete the system of equations.

The extrapolation length $\tilde{a}$ can be written in terms of the transport length λ_{tr} as

$$\tilde{a} = k_{mat}\lambda_{tr} \tag{12}$$

where k_{mat} is a parameter that depends on the material beyond the boundary point. Using the diffusion theory relation [13]

$$\lambda_{tr} = \frac{1}{\Sigma_{tr}} = 3D$$

eq 12 becomes

$$\tilde{a} = k_{mat}3D \tag{13}$$

where D is the diffusion constant. Eq 9 then becomes

$$-D\frac{d\phi/dx\big|_{x=a}}{\phi(a)} = \frac{1}{3k_{mat}} \tag{14}$$

We now define alpha as

$$\alpha = \frac{1}{3k_{mat}}$$

to get

$$-D\frac{d\phi/dx}{\phi} = \alpha \tag{15}$$

When the medium beyond the boundary is a void, then it is shown in [15] that $k_{mat} = 0.7104$. This is the solution to the “Milne Problem” which determines the neutron distribution everywhere in an infinite source-free half space with zero incident flux.

Substituting this value for k_{mat} into eq 14, we then get

$$-D\frac{d\phi/dx}{\phi} = 0.4692 \tag{16}$$

which is the result that is used in V.S.O.P.-A [16]. With this derivation, the first objective of this study is fulfilled.

Further from eq 9 and eq 15 we get that

$$\frac{\alpha}{D} = \frac{1}{\tilde{a}} \tag{17}$$

Considering Figure 3, we note that the extrapolation length for a given geometry will increase from that due to the void when a scattering material is present beyond the boundary. If a strong absorber is present beyond the boundary, this extrapolation length will decrease from that due to the void.

2.3 Physics, Limitations in Fuel Element, Reactor and Fuel Cycle

In the OTTO cycle the speed of the fuel element movement is adjusted to maintain a critical core and as a result the target burn-up can be achieved during the first pass irradiation. This type of fuel cycle doesn't require any burn-up measurement devices or refuelling equipment, which makes it more economical. The fuel is loaded in (Th+U)O_2 mixed oxide coated particles.

The reactor physics of the OTTO fuel cycle differs from other types of fuel management. Fresh fuel elements are loaded from the top, whilst the older fuel elements move to the bottom section of the reactor. The fresher and older fuel elements are not mixed to create a more homogeneous fuel mixture. There exists a power peak in the upper section of the core specifically caused by the higher fissile content of the fresh fuel being loaded. In multi-pass fuel cycles the neutron flux in the fresh fuel elements is suppressed by the poorer neutron economy in the older fuel elements which surrounds these. Therefore the power increases in these fresh fuel elements are less pronounced, but still present.

The coolant gas enters through the upper section of the reactor, removing the heat generated by the fuel element, and thus prevents the fuel element from reaching temperatures exceeding the limits of approximately 1250˚C in the centre of the fuel. In the lower section of the reactor there is hotter gas flow, but reduced power production resulting in lower heat transfer to the hot gas. It is therefore possible to increase the average gas outlet temperature up to approximately 950˚C without reaching the technological limitations [17].

When the fuel elements reach the lower section of the core, they can be regarded as having reached more than 95% of the burn-up. The influence of the neutronics of the lower core on the neutronics of the upper core is limited because of the large spatial separation between the both sections.

The radius of the power generating fuel zone affects the temperature gradient and stresses in the fuel element. There is no fabrication limit on increasing the fuel zone, but a minimum of 0.5cm thickness of the outer graphite shell is required for strength, corrosion and abrasion.

Limitations on average power density in the OTTO fuel cycle is determined by the thermal stresses in the fresh fuel in the upper section of the reactor core. In the low temperature range a maximum power of 4.5kW/sphere including a safety margin can be tolerated [1].

The increase in heavy metal loading also results in the build-up of a higher fissile inventory in the core. Radial temperature flattening can be achieved by a 2-zone fuelling of the reactor core. In this study a 1-zone configuration is assumed.

The neutron physics characteristics of the U-233 are more favourable than for U-235 in the thermal energy spectrum, and thus the displacement of U-235 by U-233 leads to positive feedback for the improvement of the conversion ratio [19].

3. CALCULATION METHODOLOGY

3.1 Introduction

When designing the reactor, models for the reactor operation using computer codes may be developed to simulate the physics characteristics of the reactor. In particular, the neutronics and thermal hydraulics of the core are modelled using V.S.O.P.-A for quasi-steady state calculations.

In this chapter, a short description of the code used in this study is given, together with the geometrical layout of the reactor as modelled in the code. Further, the execution of V.S.O.P.-A code, and changes to the input files as required for this work, is discussed.

3.2 V.S.O.P.-A Computer Code System

V.S.O.P. is a code that was originally developed in Germany to model the neutronics and thermal hydraulics of HTRs, e.g., the AVR, THTR, and HTR-Modul. It was also used by the Chinese to design the HTR-10 [20] and HTR-PM [20]. The version V.S.O.P.-A was derived from the original V.S.O.P. code.

V.S.O.P.-A is a system of proven computer codes linked together for the numerical simulation of the nuclear reactor. The calculation comprises the processing of the cross sections, reactor and fuel element design, neutron spectrum evaluation, two or three dimensional diffusion calculation, burn-up, fuel shuffling, control and, for the pebble bed HTR, thermal hydraulics of steady state and transients. Figure 4 shows the V.S.O.P. physics simulation.

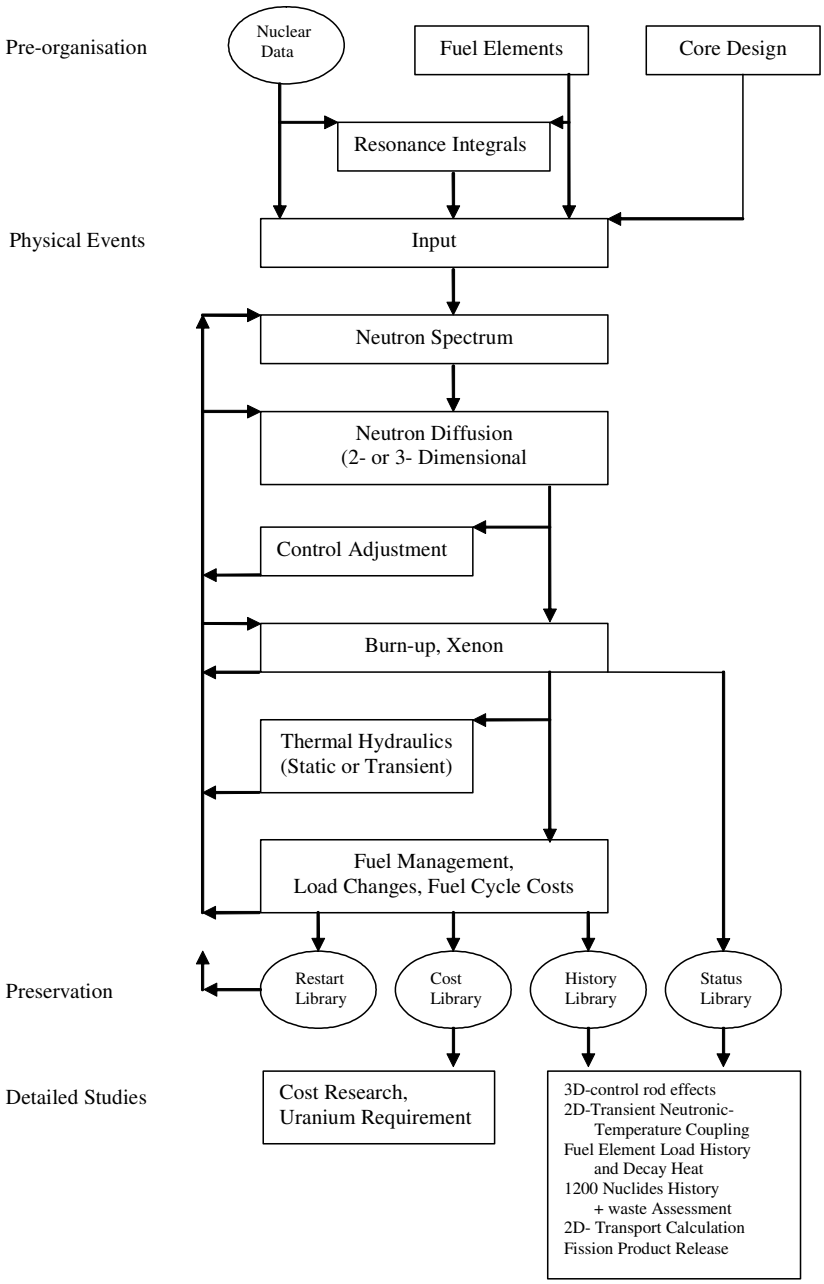


Figure 4: V.S.O.P. Physics Simulation [21]

Figure 5 shows the basic libraries and codes which V.S.O.P. is made up of.

- The two libraries GAM-I and THERMOS have been derived from the evaluated nuclear data files ENDF/B-V and JEF-1. The GAM-I library data is given in a 68 energy group structure ranging from 10 MeV through 0.414 eV. The THERMOS library data are given in 30 energy groups ranging from 10^{-5} eV through 2.05 eV.
- DATA-2 prepares the fuel element input data from its geometric design.
- BIRGIT prepares the 2-D geometric design of the reactor.
- Spectrum calculations are made by GAM-I and THERMOS for an unlimited number of spectrum zones.
- Diffusion calculations are made by the CITATION, which involves the solution of the diffusion equation.
- The burn-up and the fuel shuffling are covered by FEVER for a number of burn-up batches.
- THERMIX is included for the thermal hydraulics evaluation.

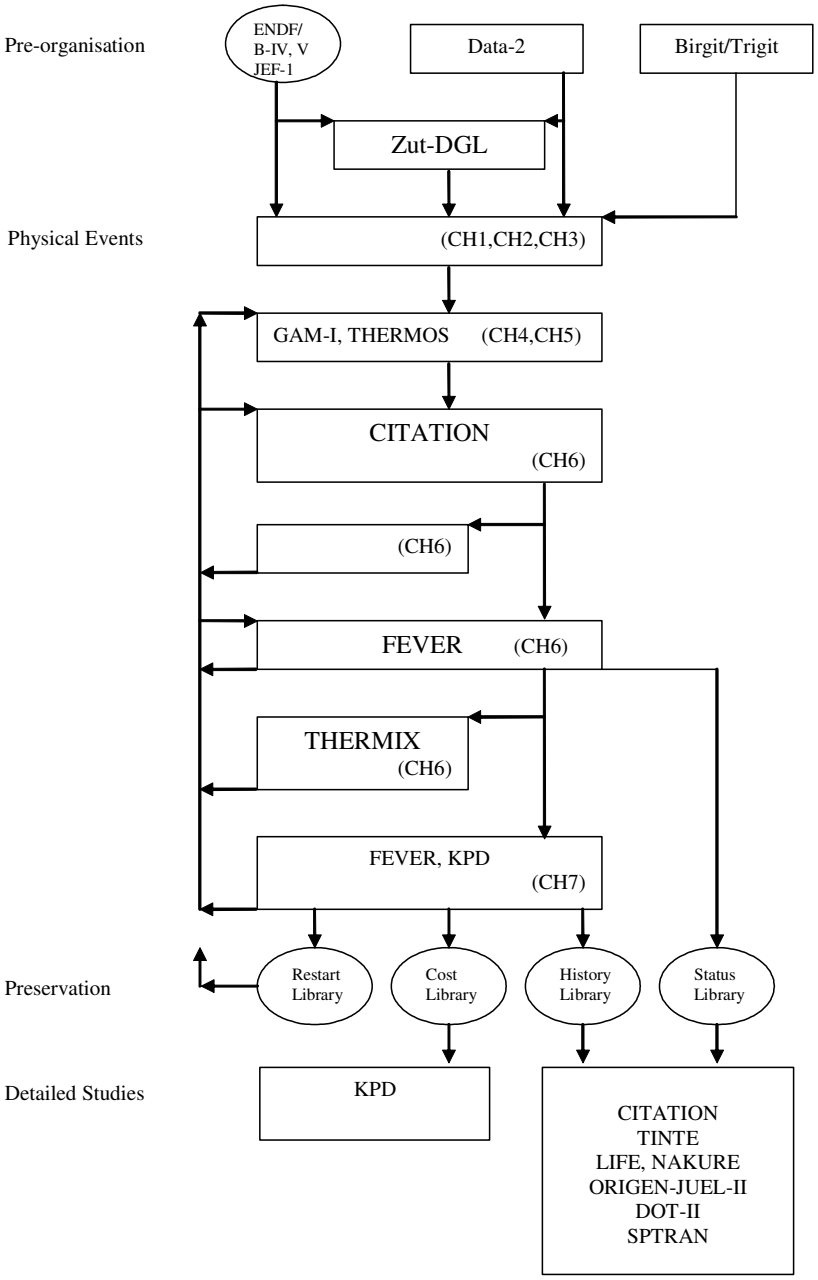


Figure 5: V.S.O.P. - The Basic Programs [21]

3.3 Geometry

The PBMR concept reactor has been conceptualized for the LEU fuel cycle of 9.6 wt % enrichment in U-235. In the reference cycle the bred fissile Pu isotopes are predominantly burnt in-situ in the reactor, and only 16 % have been estimated to appear in the spent fuel spheres.

The reactor core is annular and in Table 3 the geometrical specifications are presented of the "RUDI-1" development of the plant. This concept features the fuel elements circulating only once through the core in a so-called, OTTO cycle. The loading of about 260 spheres per day can be inserted into the core in regular intervals of one or more days. This leads to considerable simplification of the fuelling and fuel-handling features of this type of reactor.

Table 3: Geometrical Specifications of Pebble Bed Reactor 'RUDI-1'

Description	Unit	Value
Thermal power	MW_{th}	100
Core volume	m^3	25
Height / diameter	cm	503 / 260
Void thickness at the core top	cm	78.5
Height of cone at bottom	cm	57.5
Pebble passes through the core	-	1
Pattern of pebble flow (subdivided in 5 radial flow channels)	-	18 / 18 / 20 / 24 / 30
Number of control rods	-	16

3.3.1 Geometrical Layout in V.S.O.P.-A

Once the components of the reactor core and surrounding structures are selected as part of the analysis domain, these components must then be modelled geometrically in a suitable manner in a 2-D V.S.O.P.-A model [16]. The radial boundary is set at the outer side reflector edge for the neutronic

calculations including a lumped metallic portion comprised of the core barrel, RPV and void regions as indicated. This is to account for the neutron absorption in the iron.

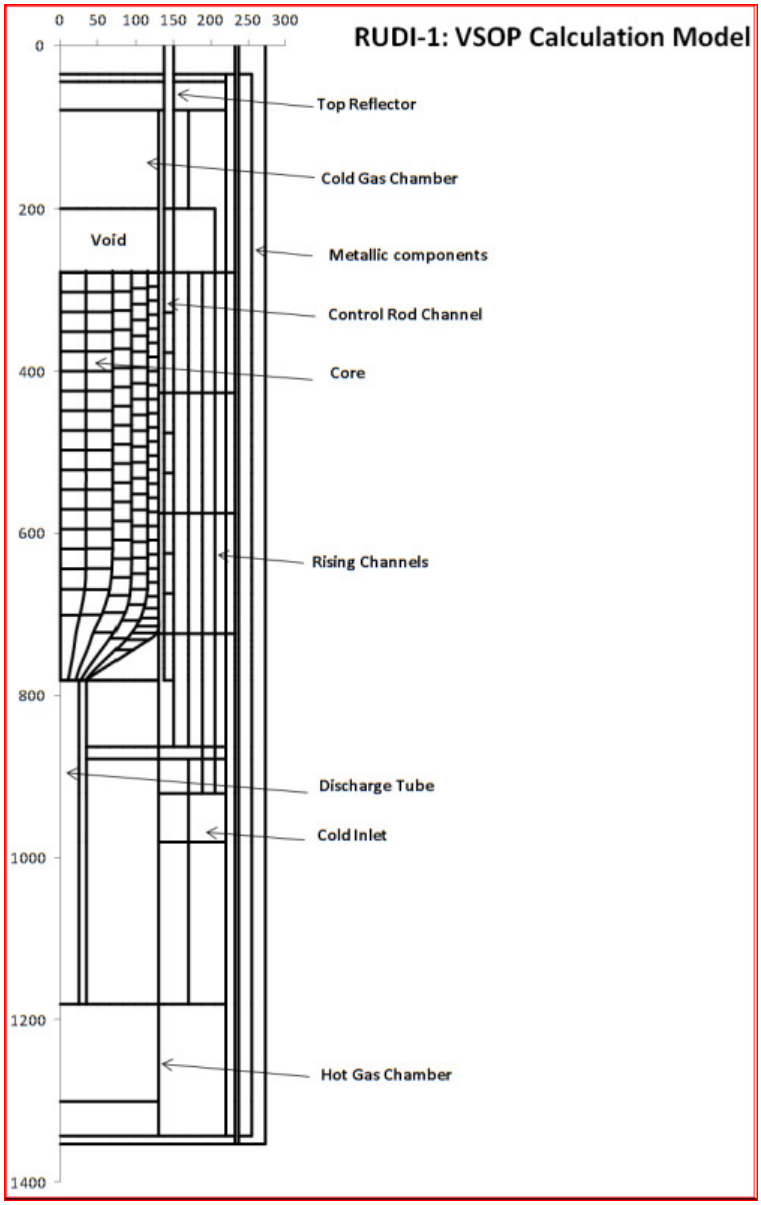


Figure 6: V.S.O.P.-A Calculation Model

3.4 Calculation Methodology

In this section, the methodologies used for the calculations performed for reactivity, burn-up, and other parameters, are presented.

In summary, this involved

- The setup of the resonance integral files with ZUT-DGL and calculation for the models;
- The volume matrix preparation;
- Determination of the reactor core layout, fuel cycle layout and calculation of the neutronics and core compositions from the start-up core through to the equilibrium cycle;
- Then follows the determination of the reactor layout for THERMIX evaluations and the restart with THERMIX run for temperature distributions. This is an iterative process to establish convergence of the cycle calculation.

3.5 Model Adjustments and Execution of Code

The project was run on a PENTIUM IV desktop personal computer using the DOS-command emulator under Windows. The input files are lengthy, and thus are not included in this report.

3.5.1 Calculation of Resonance Integrals

The resonance files were setup to calculate the resonance integral ranges for U-238 and Th-232 for the calculations to be performed.

The resonance files were setup with the following parameters as the boundary cases in order to envelope all the desired cases for investigation for both U-238 and Th-232:

1. Feed fuel enrichment from 4% to 19% and
2. Heavy metal loading from 5gHM/sphere to 20gHM/sphere.
3. Temperature ranged from 293K to 2273K with the following values
    a. 293K
    b. 673K
    c. 973K
    d. 1273K
    e. 1573K
    f. 1873K
    g. 2273K

All other Cases were naturally enveloped by the boundary cases.

As indicated above ZUT-DGL is an auxiliary program used to calculate the resonance integrals for the isotopes Th-232 and U-238 for a given isotopic concentration in the fuel assembly under consideration, and at different temperatures of the respective absorber materials. The data is stored with the background absorption cross sections of the GAM library. The code then uses interpolation to calculate the resonance integrals for temperatures and isotopic concentrations between these reference cases. These are then applied for the different spectrum calculations.

3.5.2 Execution of Resonance Integral

The files IN-DA2 and IN-ZUT are input files used to execute the ZUT-DGL batch file (SQ-ZUT) in order to determine the resonance integrals for the isotopes U-238 and Th-232. IN-DA2 gives the fuel element layout for the reactor. IN-ZUT gives the temperature range for which the resonance integrals are calculated.

The feed fuel enrichment, (card D7, ANR) and density of HM in fuel zone, (card D13, ROSM), are changed in the input file IN-DA2 for each case. No major changes to the input cards in IN-ZUT are made, except for library name.

3.5.3 Preparation of Volume Matrix

The reactor geometric design is done by preparing the volume matrix for the reactor with the auxiliary BIRGIT code.

3.5.4 Execution of Volume Matrix

The file IN-VOLMA is the input file used to execute the VOLMA batch file (SQ-VOLMA) in order to determine the volume matrix for the reactor design. The input files were standard for all cases, since the reactor design itself was not changed.

3.5.5 Calculation of V.S.O.P.-A

The criticality and the desired burn-up are adjusted by the residence time and feed fuel enrichment. The temperature adjustment is done iteratively by the THERMIX calculations run.

The above sequence of V.S.O.P.-A runs is done so that the calculation proceeds to equilibrium cycle.

3.5.6 Execution of V.S.O.P.-A

The files IN-DA2, IN-BIR and IN-HL are input files used to execute the V.S.O.P.-A batch file (SQ-HL) in order to determine the reactor physics and fuel cycle. IN-BIR gives the core layout for the reactor, whilst IN-HL is the follow to equilibrium cycle.

The feed fuel enrichment, (card D7, ANR) and density of HM in fuel zone, (card D13, ROSM), are changed in the input file IN-DA2 for each case. The IN-BIR input file is not changed.
However the IN-HL input file is changed. The card R14, namely DELDAY, which is re-definition of the length of one large time step is changed accordingly until criticality is reached.

When criticality, i.e. K_{eff} is almost close to unity, then the THERMIX calculation is run for temperature adjustment and the output file TEMPSPEK is re-entered into the IN-HL input file. Then V.S.O.P.-A is run again with the new temperature values until criticality and convergence is achieved.

3.5.7 Calculation of THERMIX

The THERMIX code is for the static and time dependent 2-D thermal hydraulics. The resulting temperature values of the fuel and of the moderator regions may be fed back to the cell calculation in each spectrum zone for subsequent core neutronics calculations.

3.5.8 Execution of THERMIX

V.S.O.P.-A is executed, and then only is the THERMIX batch file run. The files IN-BIRTH and IN-RSTX2 are input files used to execute the THERMIX batch file (SQ-RSTX2) in order to determine the temperature distribution. IN-BIRTH gives the reactor layout for THERMIX evaluations, and IN-RSTX2 is the restart with THERMIX run temperature distributions.

An output file TEMPSPEK is created. This file gives the spectrum temperature profile in the reactor core. The last set of cards namely; G2/R19 in the TEMPSPEK file is copied to replace the last set of cards G2/R19 in the IN-HL input file. Then V.S.O.P.-A is rerun with the new temperature values, i.e. the new IN-HL as input file. The criticality K_{eff} value changes with the new input file IN-HL. DELDAY is adjusted again until criticality is reached. This iteration was done for 3 runs.

4. EVALUATION OF CALCULATIONS, RESULTS AND DISCUSSION

In this chapter the calculations carried out and the results thereof will be discussed.

4.1 Extraction of Data from V.S.O.P.-A Output Files

The output files were read and tables of the valuable information created (see Appendix 7.1). This allowed easy interpretation of results and “patterns” to be observed. V.S.O.P.-A run creates the output file O-HL from which the necessary data was extracted.

4.2 Evaluation of the Calculations

The calculations for the different models listed as Cases were used to compare the output results in order to derive conclusions given the assumptions of the code and the model setup.
Case0 is the reference case of U-238 fuel cycle.
Cases 1 to 5 are the Th-232 fuel cycle cases.

Firstly the models were setup, and then cases run for different heavy metal loadings at specified feed fuel enrichment. The data entered into the tables were extracted from output files of V.S.O.P.-A. The cases for the four different feed fuel enrichments at different heavy metal loadings per fuel sphere were plotted on a single graph against a parameter under investigation.

4.3 Results and Discussion

In order to derive comparative conclusions for the Thorium fuel cycles, a Uranium fuel cycle was also performed as a reference cycle. The Uranium fuel cycle shows a high ISU of Pu isotopes of about 88 % at 9 wt % feed fuel enrichment as compared to any of the Th fuel cycles. This means that only about 12 % of the Pu isotopes are found in the spent fuel elements.

The favourable nuclear properties of the bred fissile isotope U-233 are more effective in reducing the Uranium ore requirement than U-235. This is evident in the parametric study of the Th fuel cycles. The results are shown in Table 4, Table 5, Table 6 and Table 7. The Uranium ore requirement for 20 gHM/sphere at 9 wt % feed fuel enrichment showed a 15 % less Uranium ore requirement than the Uranium cycle. However the amount of U-233 in the spent fuel that was produced during the burn-up phase is 33.5 %. This is much higher than the 12 % of Pu isotopes found in the Uranium cycle. This can be explained by the smaller thermal absorption cross-section of about 250 barn in U-233 compared to the 1100 barn in Pu-239. The recovery and recycling of the fuel with high fissile content is viable and may lead to further reductions in Uranium ore requirements in the Th cycles.

The graphical representation of the results of the Uranium ore requirement as a function of the HM loading for different feed fuel enrichments is given in Figure 7. Feed fuel enrichment of 6 wt % showed the highest Uranium ore requirement at lower HM fuel loadings. Between 12 gHM/sphere and 20 gHM/sphere, the ore requirements are within 10 % of each other. Increasing the feed fuel enrichment from 9 wt % to 18 wt % causes an increase in Uranium ore consumption at 20 gHM/sphere. However when feed fuel enrichment is decreased to 6 wt % then there is also an increase in the Uranium ore requirement. Overall the least Uranium ore requirement can be found around 20 gHM/sphere fuel loading and approximately 9 wt % enrichment.

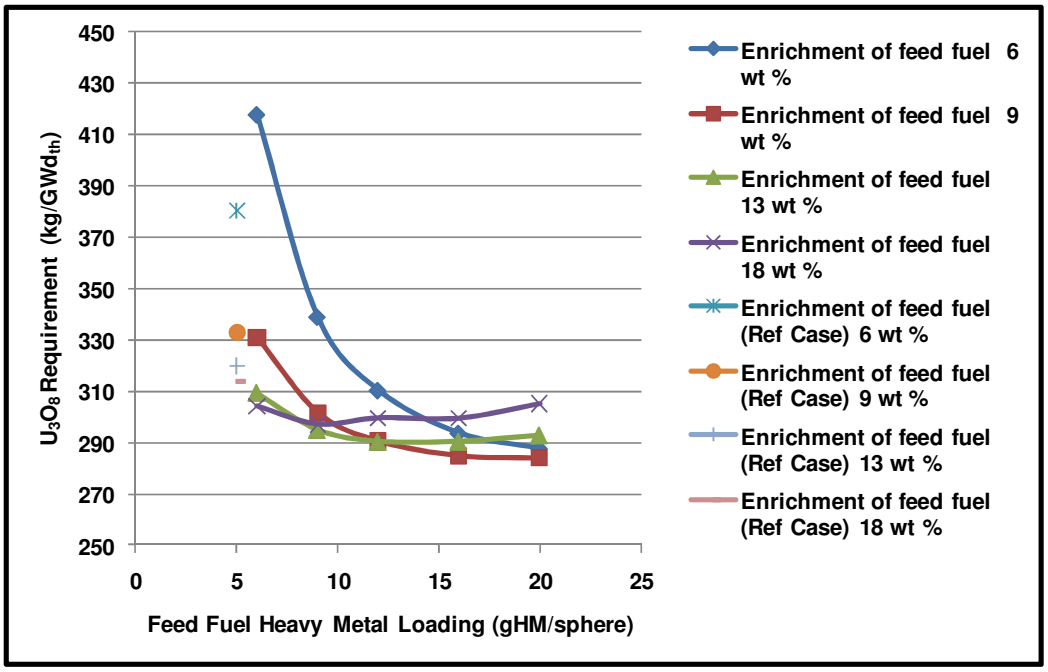


Figure 7: U_3O_8 Requirement as a function of Heavy Metal Loading

The conversion process is defined as the average number of fissile atoms produced in a reactor per fissile fuel atom consumed. As the feed fuel enrichment increases, the ratio of the fissile atoms produced per fissile atom consumed tends to decrease when the HM loading per fuel element increases. This can be seen in the gradient of the graph plot in Figure 8.

The leakage term equation (18) is an important factor in determining the conversion ratio. Factors that would increase k_{eff} also cause excess neutrons to be available for capture in Th-232 and can thus also be utilised to increase the conversion ratio in the reactor.

$$k_{eff} = k_{\infty} * P_{Non-leakage} \qquad (18)$$

The average number of neutrons emitted per thermal neutron absorbed in the fuel namely; η_T is the most important factor in the four factor formula which is given by equation (19). The moderation ratio decreases as the HM loading increases, and thus the neutrons are less ideally moderated. This results in the energy spectrum becoming harder. At some point this may cause a

serious reduction in thermal fissions of U-235 and U-233 and an increase in the radiative captures in the epithermal resonances of these isotopes, which may explain the decrease in conversion ratio.

$$k_{\infty} = \eta_{\mathrm{T}} f p \epsilon \tag{19}$$

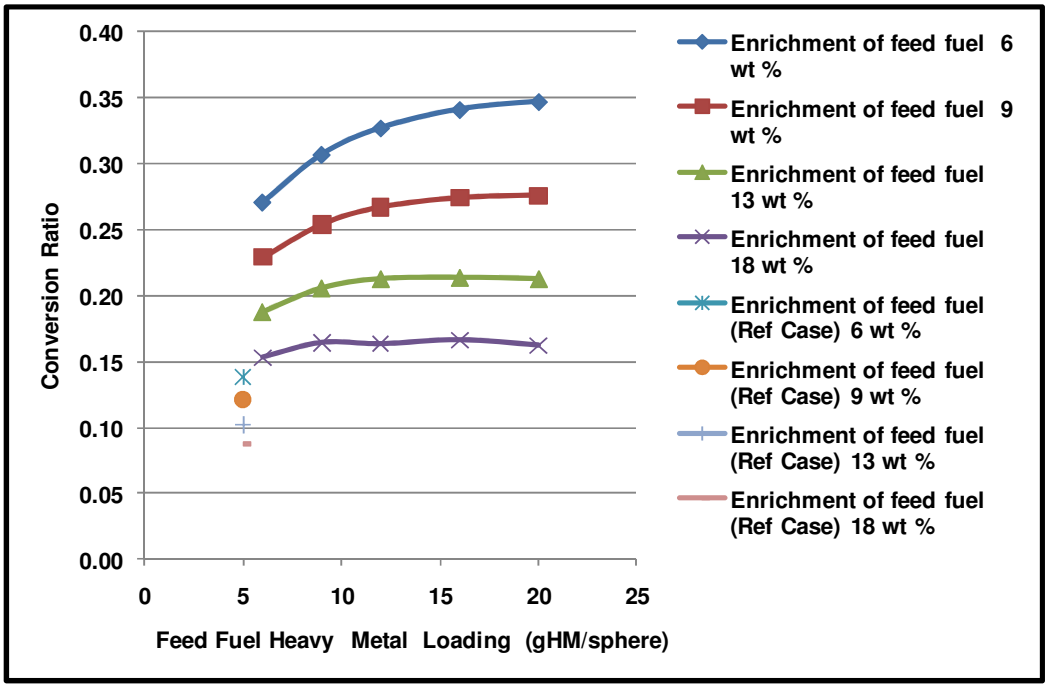


Figure 8: Conversion Ratio as a function of Heavy Metal Loading

The average burn-up reaches a maximum between 15 gHM/sphere and 20 gHM/sphere. However, the higher the feed fuel enrichment shows a greater average burn-up than the lower enrichments. The data plot is given in Figure 9. The average burn-up is also higher than the Uranium reference cycle burn-up. For the 20 gHM/sphere loading at 9 wt %, there is an approximately 18 % higher average burn-up than the U cycle.

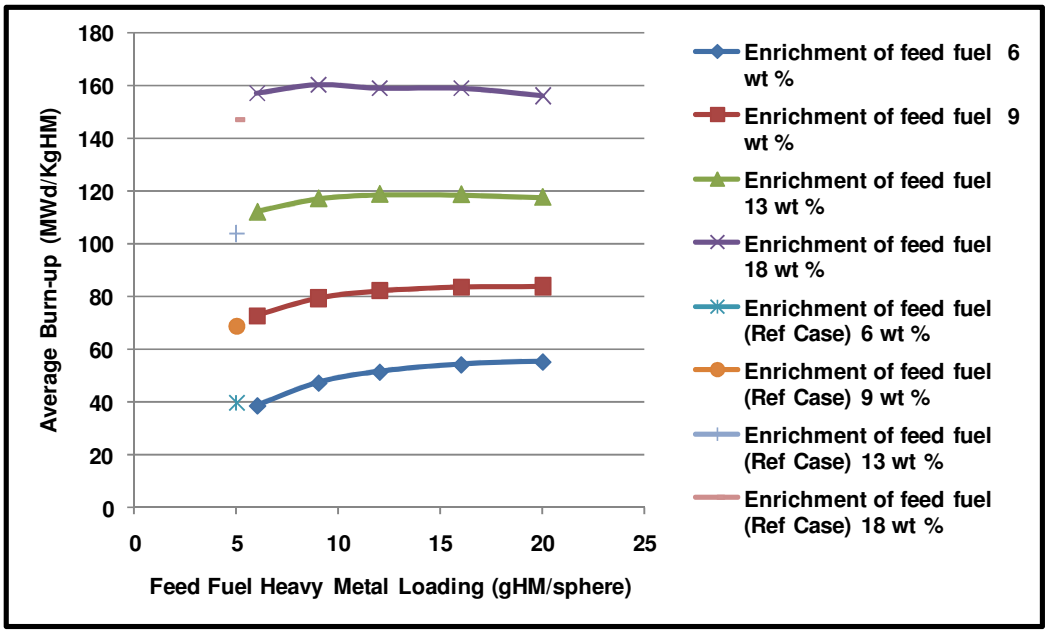


Figure 9: Average Burn up as a function of Heavy Metal Loading

The In-Situ Utilization (ISU) was calculated as follows for the **U cycle** [3]:

$$\mathrm{ISU}(Pu^{239}) = \frac{\mathrm{FA}(Pu^{239}) + \mathrm{FA}(Pu^{241})}{\mathrm{FA}(U^{238}) - \mathrm{FA}(Np^{239}) + \mathrm{FA}(Pu^{240})} \qquad (20)$$

Where FA refers to the Fractional Absorption of fission nuclides.
For the **Th cycle** one can calculate the ISU as follows [3]:

$$\mathrm{ISU}(U^{233}) = \frac{\mathrm{FA}(U^{233})}{\mathrm{FA}(Th^{232}) - \mathrm{FA}(Pa^{233})} \qquad (21)$$

Data of the ISU of bred fissile nuclides and fraction of fissions in the bred fissile nuclides is given in appendix 7.2.

The ISU of the bred fissile U-233 improves as the feed fuel enrichment is increased. The best overall ISU of 72.12 % is found at 20 gHM/sphere fuel

loading and 18 wt % feed fuel enrichment. See Figure 10 and Figure 11 for a graphical representation of the results.

Reprocessing and recycling of the fuel elements is recommended because of the relatively high fraction of U-233 in the spent fuel and also due to the favourable nuclear properties of U-233. To achieve this, the bred U-233 should be kept separate from the uranium of the feed fuel, because it contains a greater contribution of non-fissile uranium isotopes. This can be accomplished by loading the breed fuel (Th) and the feed fuel (U(93%)) into separate spheres and insert them admixed into the reactor. The loading of the case with 12 g/sphere and burn-up of 77.0 MWd/Kg could be modified into a mix of Th containing spheres with loading of 20g and U(93%) containing spheres with 2.6g/sphere in the mixing ratio of about 54% / 46%. The recovered U-233 can be used as feed fuel in a separate reactor being fuelled with U-233 / Th mixed oxide, which does not require uranium ore at all.

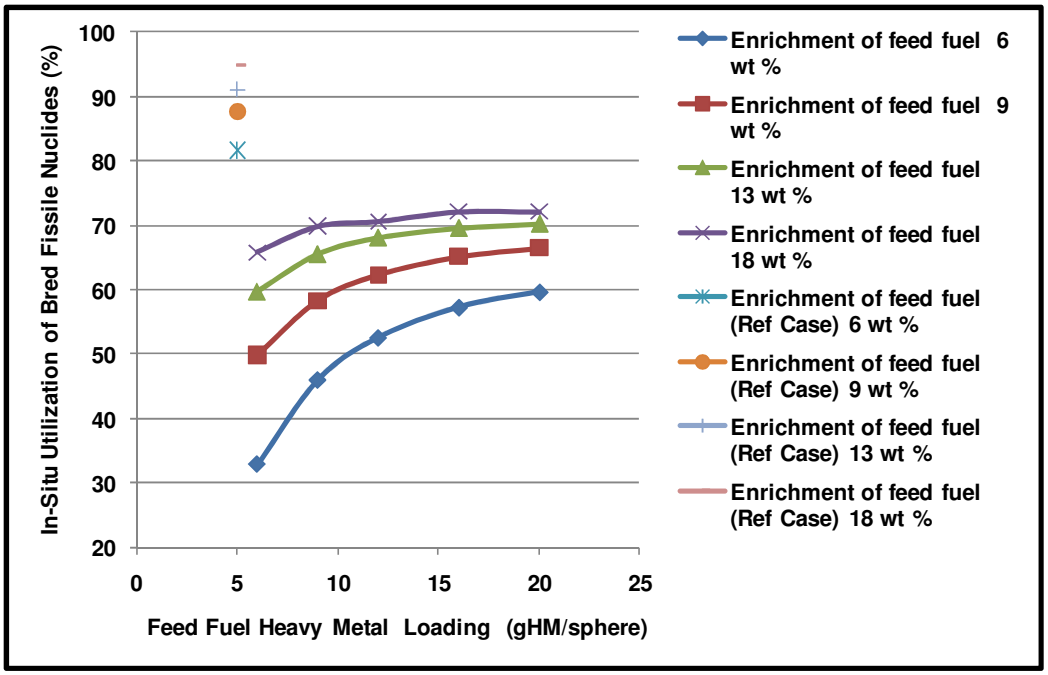


Figure 10: In-Situ Utilization of Bred Fissile Nuclides as a function of Heavy Metal Loading

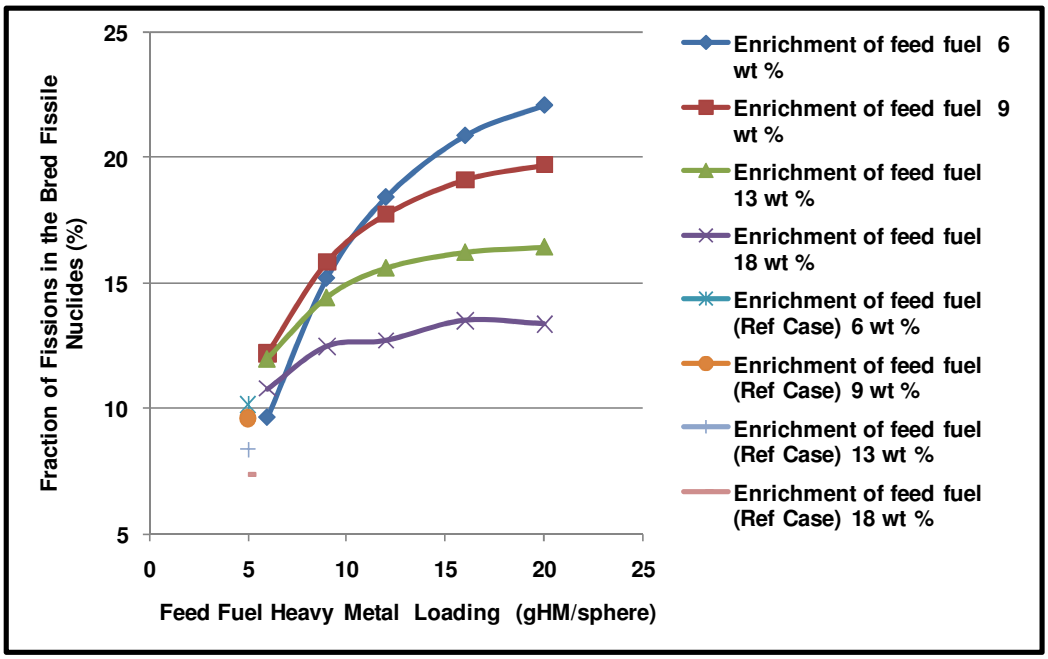


Figure 11: Fraction of Fissions in the Bred Fissile Nuclides as a function of Heavy Metal Loading

The fuel remains in the reactor for a particular period of time before it is removed as spent fuel elements. This time is referred to as the fuel residence time and is calculated in the dimension of days. The k infinity (k_∞) of the individual fuel spheres decreases with burn up. The fuel spheres with the higher heavy metal loading will produce the most burn up before their k_∞ would have decreased to a point that they have to be discarded as spent fuel. There is a linear relationship between the HM loading, associated adaptation of the level of enrichment and the fuel residence time, as the HM loading increases so does the fuel residence time.

The higher heavy metal content in the Th based fuel means higher burn up is achieved for the fuel cycle. A higher burn up would allow more of the fissile U-235 and of the Plutonium bred from the U-238 to be utilized, reducing the Uranium requirement of the fuel cycle. See Figure 12 for graphical representation of the results.

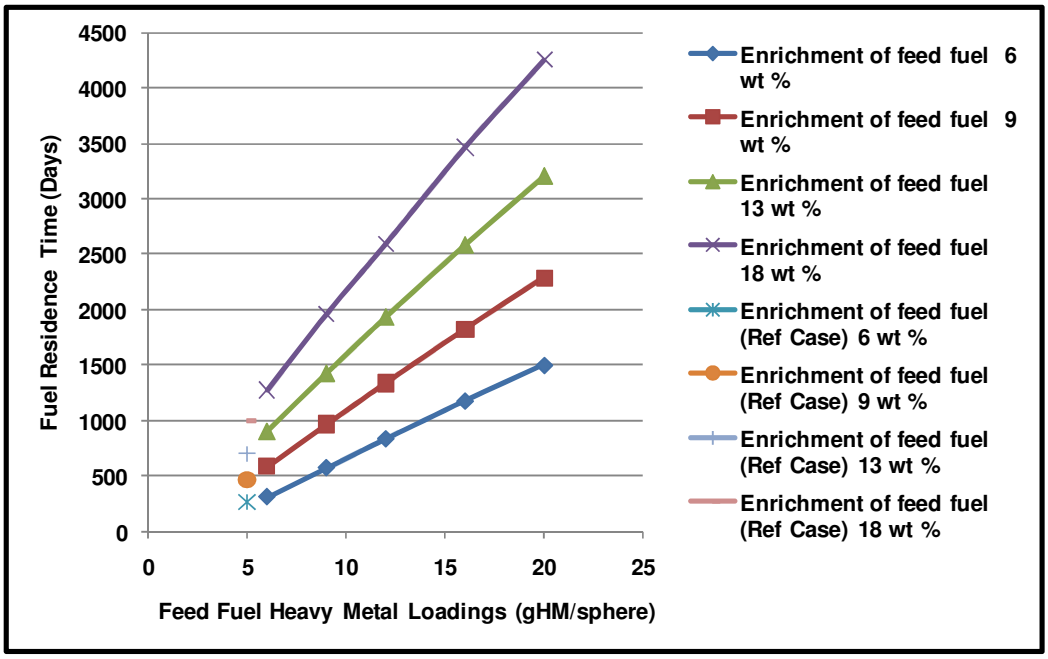


Figure 12: Fuel Residence Time as a function of Heavy Metal Loading

Table 4: Performance of U/Th Fuel Cycle at 6 wt % Feed Fuel Enrichment

		Case0	Case1	Case2	Case3	Case4	Case5
Feed Fuel Heavy Metal Loading	gHM/sphere	5	6	9	12	16	20
Moderation ratio	N_C/N_{HM}	772	627	415	310	230	180
Average Burn-up	MWd/kg_{HM}	39.47	38.38	47.10	51.30	54.11	55.18
Average Fuel Residence Time	Days	267	311	575	837	1179	1505
Conversion Ratio		0.14	0.27	0.31	0.33	0.34	0.35
U_3O_8 Requirement	kg/GWd_{th}	380	418	339	310	294	288
Separative Work	kg SWU/GWd_{th}	250	366	297	272	257	252
Loading → Unloading: U-235	kg/GWd_{th}	1.5192 - 0.3942	1.6023 - 0.4761	1.2995 - 0.2437	1.1899 - 0.1734	1.1260 - 0.1379	1.1030 - 0.1269
Unloading: U-233	kg/GWd_{th}	-	0.0000 - 0.2191	0.0000 - 0.1976	0.0000 - 0.1837	0.0000 - 0.1718	0.0000 - 0.1642
Unloading: Pu-239	kg/GWd_{th}	0.0000 - 0.0234	0.0000 - 0.0002	0.0000 - 0.0003	0.0000 - 0.0005	0.0000 - 0.0006	0.0000 - 0.0008
Unloading: Pu-241	kg/GWd_{th}	0.0000 - 0.0069	0.0000 - 0.0000	0.0000 - 0.0001	0.0000 - 0.0001	0.0000 - 0.0002	0.0000 - 0.0002
In-situ utilization of bred fissile nuclides	%	84.69	34.50	47.36	53.74	58.32	60.68
Fraction of fissions in the bred fissile nuclides	%	10.16	9.63	15.18	18.40	20.86	22.07
Fast dose	$E21/cm^{2*}360day$	1.24	1.28	1.16	1.12	1.09	1.07
Core Leakage	%	29.68	25.32	23.27	21.93	20.68	19.73
Maximum Power	kW/sphere	1.83	1.62	1.85	2.03	2.16	2.23

Table 5: Performance of U/Th Fuel Cycle at 9 wt % Feed Fuel Enrichment

		Case0	Case1	Case2	Case3	Case4	Case5
Feed Fuel Heavy Metal Loading	gHM/sphere	5	6	9	12	16	20
Moderation ratio	N_C/N_{HM}	772	627	415	310	230	180
Average Burn-up	MWd/kg_{HM}	68.52	72.55	79.21	82.09	83.65	83.86
Average Fuel Residence Time	Days	464	588	968	1340	1823	2286
Conversion Ratio		0.12	0.23	0.25	0.27	0.27	0.28
U_3O_8 Requirement	kg/GWd_{th}	333	331	302	291	285	284
Separative Work	kg SWU/GWd_{th}	238	290	264	255	249	249
Loading → Unloading: U-235	kg/GWd_{th}	1.3109 - 0.1799	1.2687 - 0.1754	1.1568 - 0.1084	1.1142 - 0.0872	1.0921 - 0.0777	1.0887 - 0.0770
Unloading: U-233	kg/GWd_{th}	-	0.0000 - 0.1355	0.0000 - 0.1239	0.0000 - 0.1168	0.0000 - 0.1107	0.0000 - 0.1066
Unloading: Pu-239	kg/GWd_{th}	0.0000 - 0.0128	0.0000 - 0.0004	0.0000 - 0.0006	0.0000 - 0.0008	0.0000 - 0.0011	0.0000 - 0.0013
Unloading: Pu-241	kg/GWd_{th}	0.0000 - 0.0048	0.0000 - 0.0001	0.0000 - 0.0002	0.0000 - 0.0002	0.0000 - 0.0003	0.0000 - 0.0004
In-situ utilization of bred fissile nuclides	%	89.91	51.40	59.51	63.40	66.12	67.53
Fraction of fissions in the bred fissile nuclides	%	9.60	12.20	15.83	17.74	19.12	19.71
Fast dose	$E21/cm^2*360day$	1.29	1.32	1.21	1.16	1.12	1.11
Core Leakage	%	29.82	26.10	24.19	22.86	21.60	20.67
Maximum Power	kW/sphere	2.38	2.17	2.43	2.54	2.61	2.64

Table 6: Performance of U/Th Fuel Cycle at 13 wt % Feed Fuel Enrichment

		Case0	Case1	Case2	Case3	Case4	Case5
Feed Fuel Heavy Metal Loading	gHM/sphere	5	6	9	12	16	20
Moderation ratio	N_C/N_{HM}	772	627	415	310	230	180
Average Burn-up	MWd/kg_{HM}	103.82	111.83	116.84	118.46	118.40	117.38
Average Fuel Residence Time	Days	704	909	1430	1936	2582	3201
Conversion Ratio		0.10	0.19	0.21	0.21	0.21	0.21
U_3O_8 Requirement	kg/GWd_{th}	320	309	295	290	290	293
Separative Work	kg SWU/GWd_{th}	241	271	258	254	254	256
Loading → Unloading: U-235	kg/GWd_{th}	1.2479 - 0.1021	1.1852 - 0.0891	1.1305 - 0.0620	1.1135 - 0.0550	1.1133 - 0.0553	1.1227 - 0.0596
Unloading: U-233	kg/GWd_{th}	-	0.0000 - 0.0879	0.0000 - 0.0815	0.0000 - 0.0776	0.0000 - 0.0742	0.0000 - 0.0717
Unloading: Pu-239	kg/GWd_{th}	0.0000 - 0.0082	0.0000 - 0.0006	0.0000 - 0.0009	0.0000 - 0.0012	0.0000 - 0.0016	0.0000 - 0.0019
Unloading: Pu-241	kg/GWd_{th}	0.0000 - 0.0032	0.0000 - 0.0002	0.0000 - 0.0003	0.0000 - 0.0004	0.0000 - 0.0005	0.0000 - 0.0006
In-situ utilization of bred fissile nuclides	%	91.99	60.99	66.47	68.96	70.46	71.23
Fraction of fissions in the bred fissile nuclides	%	8.35	11.97	14.42	15.60	16.23	16.44
Fast dose	$E21/cm^2*360day$	1.40	1.47	1.26	1.20	1.15	1.13
Core Leakage	%	29.52	26.64	24.72	23.34	21.97	21.01
Maximum Power	kW/sphere	2.78	2.64	2.86	2.95	3.06	3.14

Table 7: Performance of U/Th Fuel Cycle at 18 wt % Feed Fuel Enrichment

		Case0	Case1	Case2	Case3	Case4	Case5
Feed Fuel Heavy Metal Loading	gHM/sphere	5	6	9	12	16	20
Moderation ratio	N_C/N_{HM}	772	627	415	310	230	180
Average Burn-up	MWd/kg_{HM}	147.12	156.83	160.11	158.76	158.72	155.84
Average Fuel Residence Time	Days	1001	1278	1962	2596	3463	4250
Conversion Ratio		0.09	0.15	0.16	0.16	0.17	0.16
U_3O_8 Requirement	kg/GWd_{th}	314	304	297	300	299	305
Separative Work	kg SWU/GWd_{th}	246	266	260	262	262	267
Loading → Unloading: U-235	kg/GWd_{th}	1.2164 - 0.0588	1.1664 - 0.0541	1.1395 - 0.0422	1.1485 - 0.0461	1.1482 - 0.0458	1.1696 - 0.0549
Unloading: U-233	kg/GWd_{th}	-	0.0000 - 0.0592	0.0000 - 0.0554	0.0000 - 0.0533	0.0000 - 0.0509	0.0000 - 0.0494
Unloading: Pu-239	kg/GWd_{th}	0.0000 - 0.0058	0.0000 - 0.0009	0.0000 - 0.0013	0.0000 - 0.0016	0.0000 - 0.0021	0.0000 - 0.0025
Unloading: Pu-241	kg/GWd_{th}	0.0000 - 0.0023	0.0000 - 0.0003	0.0000 - 0.0004	0.0000 - 0.0005	0.0000 - 0.0007	0.0000 - 0.0008
In-situ utilization of bred fissile nuclides	%	93.07	66.91	70.75	71.54	73.17	73.27
Fraction of fissions in the bred fissile nuclides	%	7.34	10.79	12.47	12.70	13.49	13.35
Fast dose	$E21/cm^{2*}360day$	1.64	1.73	1.46	1.33	1.24	1.19
Core Leakage	%	29.57	26.85	24.83	23.00	21.99	20.96
Maximum Power	kW/sphere	3.26	3.07	3.30	3.34	3.55	3.63

The cost of enriching Uranium is described in terms of a special unit called the Separative Work Unit (SWU). It requires the separation of the two isotopes U-235 and U-238 which have nearly the same atomic weight. This means that work must be performed in order to separate these two isotopes. The U cycle has a separative work requirement of 237.8 SWU/GWdth and the Th cycle 248.6 SWU/GWdth at 20 gHM/sphere. This is a mere 4 % more requirement than the U cycle. It may be of interest to consider the variation of feed and separative work requirements with the residual enrichment of the tails. At fixed values of feed enrichment and product enrichment the feed requirements decrease with decreasing tail enrichments [11]. The desire to change tails enrichment is dependent on (i) the relative costs of separative work and Uranium feed and (ii) the interest to conserve natural Uranium resources.

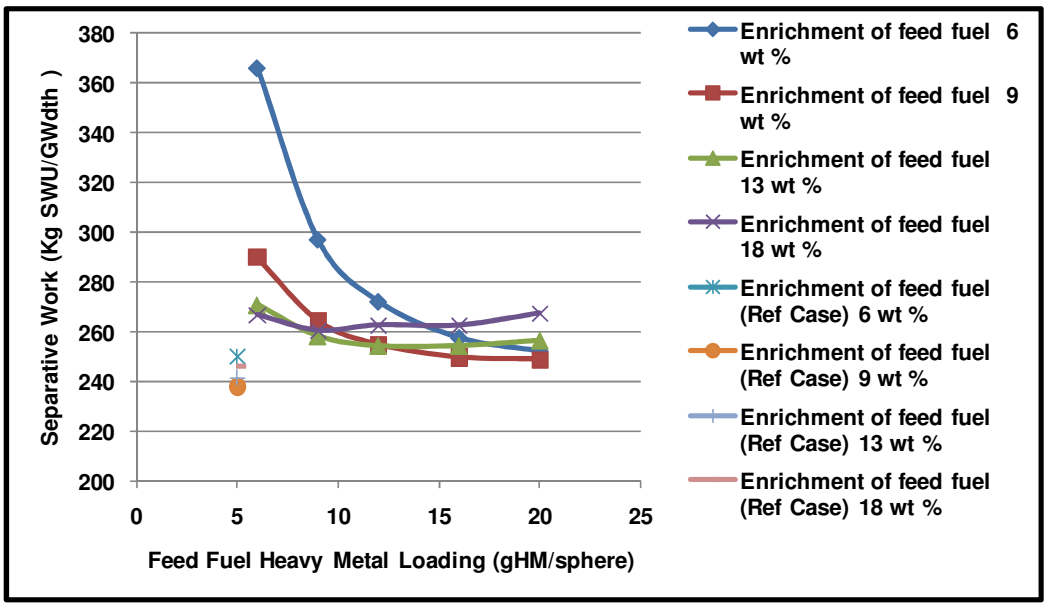


Figure 13: Separative Work as a function of Heavy Metal Loading

The core leakage in the U cycle is about 30 % higher than the leakage in the Th cycles. The higher HM loadings showed the least core leakage of 20 % as compared to the 30 % seen in the U cycle. See Figure 14 for graphical representation.

Majority of the neutron leakage occurs via the capture of thermal neutrons in: (a) the graphite in the reflectors, and (b) the control rods. Thus, in order to enter the reflectors, the neutrons must first escape the useful capture by the Th or by fission absorption by the U in the fuel and the fission products. The higher the heavy metal content of the fuel spheres, the greater the probability of being absorbed in the fuel and thus the probability for being captured in the reflectors becomes lower. The higher the fissile U loading for the neutrons that remain in the fuel, the higher is the probability for these thermal neutrons to be absorbed for fission and thus the probability of being captured by the fission products becomes lower.

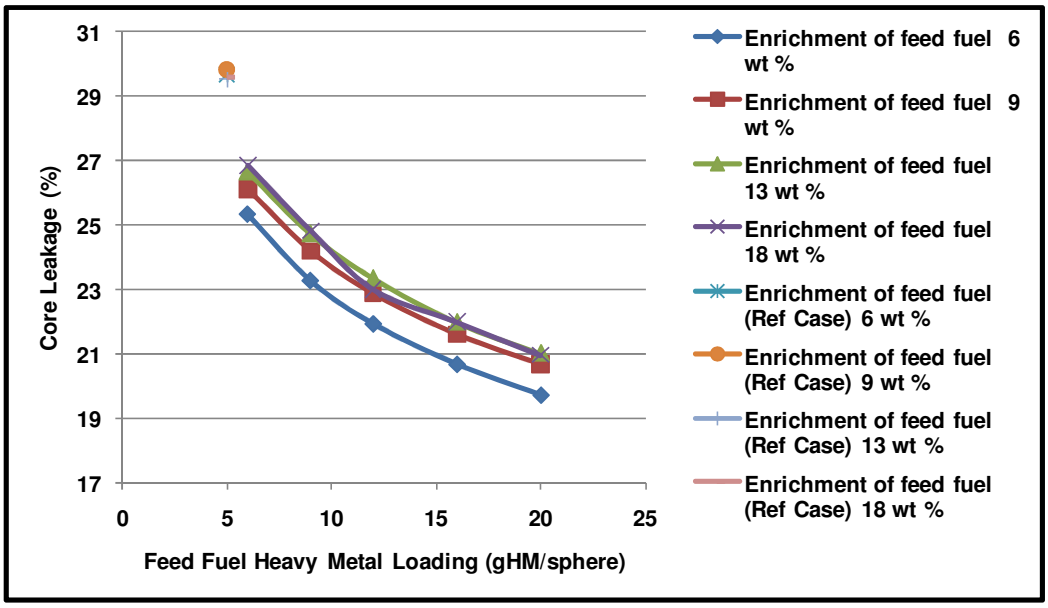


Figure 14: Core Leakage as a function of Heavy Metal Loading

4.4 Discussion Summary

At the start-up phase of the U/Th fuel cycle is advisable to insert the high enriched Uranium and Thorium as a mixed oxide in fuel spheres of 20 gHM/sphere at 9 wt % feed enrichment which will result in a burn-up of 77 MWd/kg_{HM}. The Uranium ore requirement for this specification is 15 % less than that required by Uranium cycle.

The cycles can be closed by reprocessing and recycling in order to utilise the high U-233 isotope content in the spent fuel elements. The Thorium and enriched Uranium should be loaded in separate fuel elements, which enable separate recovery of the fissile U-233 isotope.

The U-233 fissile isotope can be used as feed fuel in another reactor that is operated in a U-233/Th cycle. This means that no Uranium ore will be required and thus implies that the resource can be conserved for future use.

5. CONCLUSIONS AND RECOMMENDATIONS

It is evident from the study that the 20 gHM/sphere at 9 wt % feed enrichment fuel cycle is the optimal cycle when compared to the Uranium reference cycle and the other HM loadings. It resulted in a saving of 15 % of the required Uranium ore compared to the U cycle.

However, depending on the manufacturing processes used there might exist a risk of coated fuel particles being crushed due to higher packing fraction as the heavy metal loading is increased to 20 gHM/sphere. The benefit associated with going above this HM loading must be clearly justified. At higher burn-up the quality neutron economy of U-233 is impacted.

Further work resulting from this study would be to vary the target burn-up in close consideration of the feedback due to temperature effects. The impact of decay heat due to the presence of Protactinium has not been included in this study. Switching to a lower burn-up which is favourable for a closed cycle, would also improve the quality of the fissile isotope U-233.

Another possible investigation would be to evaluate whether the U-233 can be utilized as feed fuel in a similar reactor layout but operated as a U-233/Th cycle without U_3O_8 requirement.

6. BIBLIOGRAPHY

[1] IAEA-Nuclear Energy Agency, *Uranium 2007: Resources, Production and Demand,* June 2008

[2] World Nuclear Association, *Thorium*, February 2009, www.world-nuclear.org/info/inf62.html

[3] Mulder E., *Study Proposal: Th-Fuel Cycle in a 100MWth Pebble Bed HTR,* Potchefstroom, 22 September 2009

[4] Fenech, H., *Heat Transfer and Fluid Flow in Nuclear Systems*, Pergamon Press,1980, p382-401

[5] Kasten P.R., et. al., *Design Concepts for the Core Structure of a MOSEL (Molten Salt Experimental) Reactor*, Nuclear Structural Engineering 2 (1965), Report Number 2244-232

[6] IAEA-TECHDOC-1450, *Thorium fuel cycle – Potential benefits and challenges*, May 2005

[7] http://en.wikipedia.org/wiki/Thorium_series#Thorium_series

[8] http://en.wikipedia.org/wiki/Uranium_series#Uranium_series

[9] NUREG/CR-6839, ORNL/TM-2003/223, *Fort Saint Vrain Gas Cooled Reactor Operational Experience*

[10] Schenk W., Verfondern K., & Nabielek H. Toscano E.H., *Limits of LEU TRISO Particle Performance*, Germany

[11] Lamarsh R.J., Baratta A.J., *Introduction to Nuclear Engineering,* 3rd edition, Prentice Hill, New Jersey, 2001, ISBN 0-201-82498-1

[12] Duderstadt J.J, Hamilton L.J, *Nuclear Reactor Analysis*, John Wiley and Sons, New York, 1976, ISBN 0-471-22363-8

[13] Stacey W.M., *Nuclear Reactor Physics*, John Wiley and Sons, NY, 2001, ISBN 0-471-39127-1

[14] Fowler T.B., et.al., *Nuclear Reactor Core Analysis Code: CITATION*, ORNL-TM-2496, Rev. 2, Oak Ridge National Laboratory, Tennessee, October 1971

[15] Case K. M., Zweifel P. F., *Linear Transport Theory*, Addison-Wesley, Massachusetts, 1967

[16] Mulder E., Teuchert E., *V.S.O.P.-A Computer Code System for Reactor Physics and Fuel Cycle Simulation*, 2006

[17] Hansen U., Schulten R., Teuchert E., *Physical Properties of the "Once Through Then Out" Pebble-Bed Reactor*, Nuclear Science and Engineering: 47, 132-139, 1972

[18] Teuchert E., Rütten H.J., et.al., *Closed Thorium Cycles in the Pebble Bed HTR*, KFA, Jul 1569, ISSN 0366-0885

[19] Teuchert E., & Haas K.A., *Parametric Study on the Closed Thorium Fuel Cycle*, Germany, 1978

[20] Jing X, *et.al.*, *Predictions calculations and experiments for the first criticality of the 10 MW High Temperature Gas cooled reactor test module*, Nuclear Engineering and Design, 218 , pg 43 – 49, 2002

[21] Rütten H J, Haas K A, *VSOP. (99/3) – Update 2, PBMR- Version*, Jül-2897, Forshungszentrum Julich, July 2004

7. APPENDICES

7.1 Appendix A: Data for Fuel Supply and Discharge

		Case0		Case1		Case2		Case3		Case4		Case5	
		U238		Th232		Th232		Th232		Th232		Th232	
	Feed fuel heavy metal loading (gHM/sphere)	5		6		9		12		16		20	
Enrichment of feed fuel (wt %)	Fuel Supply and Discharge	Kg/GWd$_{th}$											
6	Loading → unloading: U-235	1.5192	0.3942	1.6023	0.4761	1.2995	0.2437	1.1899	0.1734	1.1260	0.1379	1.1030	0.1269
	Unloading: U-233	-	-	0.0000	0.2191	0.0000	0.1976	0.0000	0.1837	0.0000	0.1718	0.0000	0.1642
	Unloading: Pu-239	0.0000	0.0234	0.0000	0.0002	0.0000	0.0003	0.0000	0.0005	0.0000	0.0006	0.0000	0.0008
	Unloading: Pu-241	0.0000	0.0069	0.0000	0.0000	0.0000	0.0001	0.0000	0.0001	0.0000	0.0002	0.0000	0.0002
9	Loading → unloading: U-235	1.3109	0.1799	1.2687	0.1754	1.1568	0.1084	1.1142	0.0872	1.0921	0.0777	1.0887	0.0770
	Unloading: U-233	-	-	0.0000	0.1355	0.0000	0.1239	0.0000	0.1168	0.0000	0.1107	0.0000	0.1066
	Unloading: Pu-239	0.0000	0.0128	0.0000	0.0004	0.0000	0.0006	0.0000	0.0008	0.0000	0.0011	0.0000	0.0013
	Unloading: Pu-241	0.0000	0.0048	0.0000	0.0001	0.0000	0.0002	0.0000	0.0002	0.0000	0.0003	0.0000	0.0004
13	Loading → unloading: U-235	1.2479	0.1021	1.1852	0.0891	1.1305	0.0620	1.1135	0.0550	1.1133	0.0553	1.1227	0.0596
	Unloading: U-233	-	-	0.0000	0.0879	0.0000	0.0815	0.0000	0.0776	0.0000	0.0742	0.0000	0.0717

		Case0		Case1		Case2		Case3		Case4		Case5	
		U238		Th232		Th232		Th232		Th232		Th232	
	Feed fuel heavy metal loading (gHM/sphere)	5		6		9		12		16		20	
Enrichment of feed fuel (wt %)	Fuel Supply and Discharge	Kg/GWd_{th}											
	Unloading: Pu-239	0.0000	0.0082	0.0000	0.0006	0.0000	0.0009	0.0000	0.0012	0.0000	0.0016	0.0000	0.0019
	Unloading: Pu-241	0.0000	0.0032	0.0000	0.0002	0.0000	0.0003	0.0000	0.0004	0.0000	0.0005	0.0000	0.0006
18	Loading → unloading: U-235	1.2164	0.0588	1.1664	0.0541	1.1395	0.0422	1.1485	0.0461	1.1482	0.0458	1.1696	0.0549
	Unloading: U-233	-	-	0.0000	0.0592	0.0000	0.0554	0.0000	0.0533	0.0000	0.0509	0.0000	0.0494
	Unloading: Pu-239	0.0000	0.0058	0.0000	0.0009	0.0000	0.0013	0.0000	0.0016	0.0000	0.0021	0.0000	0.0025
	Unloading: Pu-241	0.0000	0.0023	0.0000	0.0003	0.0000	0.0004	0.0000	0.0005	0.0000	0.0007	0.0000	0.0008

7.2 Appendix B: Data for ISU and Fraction of Fissions in Bred Fissile Nuclides

		Case0	Case1	Case2	Case3	Case4	Case5
		U238	Th232	Th232	Th232	Th232	Th232
	Feed fuel heavy metal loading (gHM/sphere)	5	6	9	12	16	20
Enrichment of feed fuel (wt %)		%					
6	In-situ utilization of bred fissile nuclides	81.64	32.83	45.96	52.53	57.23	59.63
	Fraction of fissions in the bred fissile nuclides	10.16	9.63	15.18	18.40	20.86	22.07
9	In-situ utilization of bred fissile nuclides	87.66	49.87	58.33	62.34	65.12	66.49
	Fraction of fissions in the bred fissile nuclides	9.60	12.20	15.83	17.74	19.12	19.71
13	In-situ utilization of bred fissile nuclides	91.11	59.68	65.47	68.03	69.50	70.17
	Fraction of fissions in the bred fissile nuclides	8.35	11.97	14.42	15.60	16.23	16.44
18	In-situ utilization of bred fissile nuclides	94.88	65.81	69.84	70.62	72.14	72.12
	Fraction of fissions in the bred fissile nuclides	7.34	10.79	12.47	12.70	13.49	13.35